JHEP

Published for SISSA by Springer

Received: *September 18, 2012*
Revised: *October 26, 2012*
Accepted: *November 6, 2012*
Published: *November 23, 2012*

A fast track towards the 'Higgs' spin and parity

John Ellis,[a,b] **Dae Sung Hwang,**[c] **Verónica Sanz**[b,d] **and Tevong You**[a,b]

[a] *Theoretical Particle Physics and Cosmology Group, Physics Department, King's College London, Strand, London, U.K.*

[b] *Theory Division, Physics Department, CERN, CH-1211 Geneva 23, Switzerland*

[c] *Department of Physics, Sejong University, Seoul 143747, South Korea*

[d] *Department of Physics and Astronomy, York University, Toronto, ON, M3J 1P3, Canada*

E-mail: john.ellis@cern.ch, dae.sung.hwang@cern.ch, vsanz@yorku.ca, tiann.tevong.you@cern.ch

Abstract: The LHC experiments ATLAS and CMS have discovered a new boson that resembles the long-sought Higgs boson: it cannot have spin one, and has couplings to other particles that increase with their masses, but the spin and parity remain to be determined. We show here that the 'Higgs' + gauge boson invariant-mass distribution in 'Higgs'-strahlung events at the Tevatron or the LHC would be very different under the $J^P = 0^+, 0^-$ and 2^+ hypotheses. Our analysis is based on simulations of the experimental event selections and cuts using `PYTHIA` and `Delphes`, and incorporates statistical samples of 'toy' experiments. The observation of 'Higgs'-strahlung at the Tevatron and the expected peaking of backgrounds at low invariant masses suggest that this process could provide a fast-track indicator of the 'Higgs' spin and parity.

Keywords: Higgs Physics, Beyond Standard Model

ArXiv ePrint: 1208.6002

JHEP11(2012)134

doi:10.1007/JHEP11(2012)134

Contents

1 Introduction

The new particle X with mass $\sim$ 125 to 126 GeV that has been discovered by the LHC experiments ATLAS [1] and CMS [2], with support from the TeVatron experiments CDF and D0 [3], has similarities to the long-sought Higgs particle H. The X particle is a boson that does not have spin one, and its couplings to other particles depend on their masses in a way very similar to the linear dependence expected for the Higgs boson of the Standard Model [4]. However, the spin and parity J^P of the X particle remain to be determined, and this should be regarded as an open question, with the pseudoscalar hypothesis $J^P = 0^-$ and the tensor hypothesis $J^P = 2^+$ being important possibilities to exclude.

Various strategies have been proposed for determining the spin and parity of a Higgs candidate in hadron-hadron collisions, including angular distributions and kinematic correlations in $X \to ZZ^*, WW^*$ and $\gamma\gamma$ decays [5–22]. Historically, the problem of determining the spin and parity of a Higgs candidate was first considered in the context of e^+e^- collisions, and the point was made that the threshold behaviour of the cross section for the 'Higgs'-strahlung process $e^+e^- \to Z + X$ would depend on the spin and parity of the X particle, offering potential discrimination between different spin-parity assignments [23].

In this paper we point out that calculations of the $V + X$ invariant mass distributions in antiproton-proton collisions at the Tevatron collider and proton-proton collisions at the LHC reflect these differences in threshold behaviour. In particular, the mean invariant mass $\langle M_{VX} \rangle$, as calculated using `HELAS` [24] and `MadGraph` [25], would be very different in the $J^P(X) = 0^+, 0^-$ and 2^+ cases, where we assume graviton-like couplings in the latter case.

JHEP11(2012)134

Specifically, we find in both parton-level simulations using PYTHIA [26] and more detailed detector simulations using Delphes [27] that $\langle M_{VX(0^+)}\rangle \ll \langle M_{VX(0^-)}\rangle \ll \langle M_{VX(2^+)}\rangle$, also after applying the experimental event selections and cuts. We use statistical samples of 'toy' experiments to analyze the potential discriminating power of the TeVatron and LHC experiments. These demonstrate that they may (soon) be able to discriminate between different J^P assignments for the X particle using the $V + X$ invariant mass distribution. The TeVatron experiments have observed 'Higgs'-strahlung with $\sim 3-\sigma$ significance [3], and the backgrounds are expected to peak at low invariant masses, giving hope that this mechanism could provide a 'fast track' towards determining its spin and parity.

2 Calculations for different spin-parity assignments

The fact that the X particle has been observed to decay into a pair of on-shell photons implies, as is well known, that it cannot have spin one. The simplest possibilities are that it has spin zero or spin two, both of which occur in some theoretical frameworks. For example, there are many proposals for particles with the pseudoscalar assignment $J^P = 0^-$, as well as the assignment 0^+ expected for the Higgs boson of the Standard Model, and models postulating extra dimensions raise the possibility of a massive spin-two particle.

In the case of the 0^+ assignment for the X particle, we assume the minimal $V_\mu V^\mu X$ coupling, and in the 0^- case we assume the dimension-five effective coupling $\epsilon_{\mu\nu\rho\sigma}F^{\mu\nu}F^{\rho\sigma}X$, where $F_{\mu\nu}$ is the field-strength tensor of the vector boson V. In the case of a spin-two X particle, there is considerable ambiguity in the possible couplings, with a five-parameter set of possibilities considered in [23] for the 2^+ assignment, and a set of four possibilities for the 2^- case. We study the option that we consider the best motivated, namely the 2^+ assignment with graviton-like couplings to all other particles including vector bosons.[1] We use in our simulations the HELAS library [24], including its implementation of a massive spin-two particle with graviton-like couplings, and generate its production and decays using MadGraph. We implemented the pseudo-scalar couplings to gauge bosons and fermions, as well as Feynrules [28] and the UFO model format [29] for implementation into Madgraph.

As already mentioned, the reaction $e^+e^- \to Z + X$ was shown in [23] to exhibit significant differences in the energy dependence of the total cross section for X production in the $J^P = 0^{+,-}, 2^+$ cases, and other possible J^P assignments were also considered. Here we apply the considerations of [23] to the related processes $\bar{p}p, pp \to \{Z, W\} + X$. Discriminating power is provided by the threshold behaviour of the cross section. We recall that production is an s-wave process in the 0^+ case, so that the cross section rises $\sim \beta$ close to threshold. In the 0^- case, on the other hand, the production mechanism is p-wave, and the threshold behaviour $\sim \beta^3$. In the 2^+ case, many of the possible couplings make d-wave contributions to $V + X$ production amplitudes, yielding contributions to the total cross section $\sim \beta^5$, and these contributions dominate in the case of graviton-like couplings.

[1] We note that Lorentz invariance and Standard Model gauge symmetries forbid dimension-four couplings of a massive spin-two particle, and that the flavour and CP symmetries of the Standard Model require it to couple flavour-diagonally to other particles via dimension-five terms that take the same forms as their energy-momentum tensors [30].

JHEP11(2012)134

Figure 1 compares the (arbitrarily normalized) $Z + X$ invariant mass (M_{ZX}) distributions in the $J^P = 0^+$ case (solid black lines), the $J^P = 0^-$ case (dotted pink lines) and the graviton-like $J^P = 2^+$ case (dashed blue line) cases at the TeVatron (left panel) and at the LHC at 8 TeV (right panel), as simulated using `MadGraph` [25] and `PYTHIA` [26] at the parton level without including any detector simulation. The results for the different spin-parity assignments are clearly very different, yielding large differences in the mean values of $\langle M_{ZX} \rangle$. At the parton level, we find the following values for the distances above threshold, $\langle M_{ZX} \rangle - M_Z - M_X$, in the $J^P = 0^+, 0^-$ and 2^+ cases:

$$\begin{array}{rlll} & & \text{TeVatron} & \text{LHC at 8 TeV} \\ & (0^+) & 75 \text{ GeV}; & 88 \text{ GeV} \\ \langle M_{ZX} \rangle - M_Z - M_X = & (0^-) & 194 \text{ GeV}; & 303 \text{ GeV} \\ & (2^+) & 400 \text{ GeV}; & 1340 \text{ GeV} \, . \end{array} \tag{2.1}$$

For comparison, we note that the invariant mass distributions for the $Z + \bar{b}b$ background, shown as the green histograms in figure 2 for the TeVatron using the D0 cuts described below (left panel) and the LHC at 8 TeV using the CMS cuts also described below (right panel), are sharply peaked towards low invariant masses close to threshold, even closer than the $J^P = 0^+$ case (2.1). The backgrounds due to VV and $\bar{t}t$ production are also expected to peak at low invariant masses.

Encouraged by the differences seen in (2.1) and in figure 1, we have made simulations of the possible signals in the TeVatron and LHC experiments. We have not analyzed further the backgrounds in the experiments, which would require more extensive simulations beyond the scope of this work, in particular because [3] gives no details of the MVA analyses used by CDF and D0 in extracting evidence for 'Higgs'-strahlung. However, we note that figure 2 indicates that the backgrounds would be negligible if the X particle has $J^P = 2^+$, and would also have a very different M_{ZX} distribution from a 0^- signal. The signal and backgrounds would be more similar in the 0^+ case, but figure 2 of [3] indicates that the statistical uncertainty in the background is small for $\log_{10}(s/b) > -1.5$ also in the 0^+ case.

3 Detector simulations for different spin-parity assignments

3.1 TeVatron

The TeVatron experiments CDF and D0 have reported evidence for production of the X particle in association with $Z \to \ell^+\ell^-, \bar{\nu}\nu$ and $W^\pm \to \ell^\pm \nu$ [3]. In this section we simulate these analyses using `Delphes`. We first apply the following baseline parton-level cuts at the generator level: $p_T^\ell > 10\,\text{GeV}$, $|\eta_\ell| < 2.$, $p_T^j > 20\,\text{GeV}$, $|\eta_j| < 2.5$ and $\Delta R_{j\ell} > 0.5$, where η is the pseudo-rapidity and R is the standard cone angle variable, and jets are reconstructed using the cone size $R = 0.5$ As shown in the left panel of figure 3, the discrimination between the different possible spin-parity assignments survives the baseline cuts. We next proceed to implement event selections and cuts specific to the CDF and D0 experiments for analyses with two, one and zero leptons.

JHEP11(2012)134

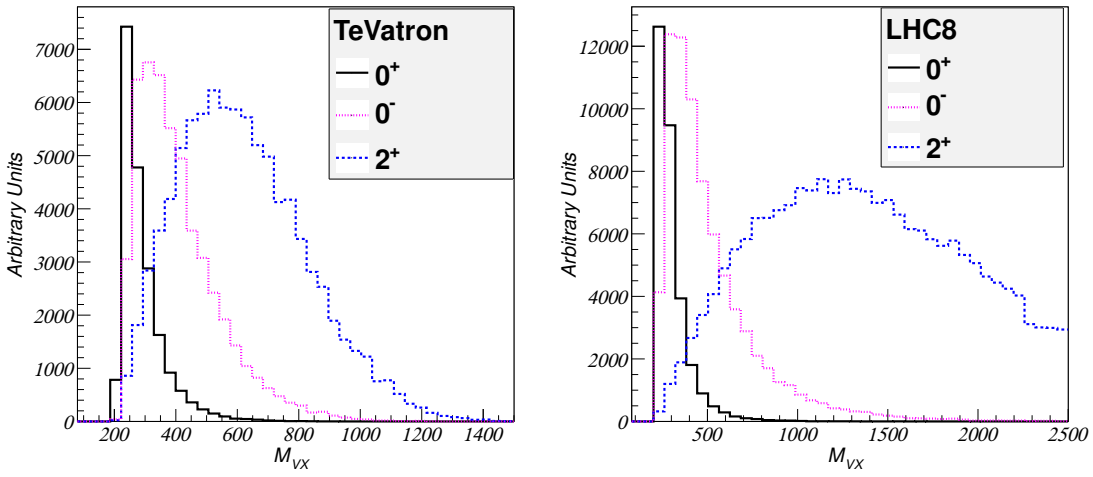

Figure 1. The distributions in the $Z + X$ invariant mass M_{ZX} for the 0^+ (solid black), 0^- (pink dotted) and 2^+ (blue dashed) assignments for the particle X with mass $\sim 125\,\text{GeV}$ discovered by ATLAS [1] and CMS [2], calculated for the reaction $\bar{p}p \to Z + X$ at the TeVatron (left) and for the reaction $pp \to Z + X$ at the LHC at 8 TeV (right).

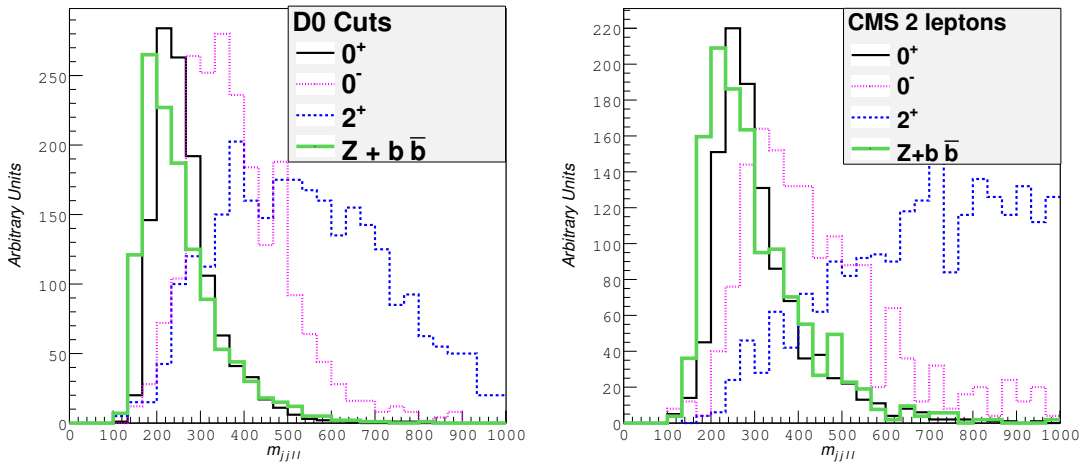

Figure 2. The $Z + \bar{b}b$ background invariant mass distribution (green) at the TeVatron using the D0 cuts described in the text (left panel) and the LHC at 8 TeV using the CMS cuts also described in the text (right panel) compared with the two-lepton signal distributions in the $Z + X$ invariant mass M_{ZX} for the 0^+ (solid black), 0^- (pink dotted) and 2^+ (blue dashed) assignments for the particle X with mass $\sim 125\,\text{GeV}$.

3.1.1 D0 and CDF $Z \to \ell^+\ell^- + X \to \bar{b}b$ analyses

The D0 [31] selection cuts we implement are different for muons and electrons. In the muon case, we ask for a leading lepton with p_T >20 GeV and $|\eta_\ell| < 2$, and a sub-leading lepton with $p_T > 15\,\text{GeV}$ and $|\eta_\ell| < 1.5$. The electron category is characterized by two

JHEP11(2012)134

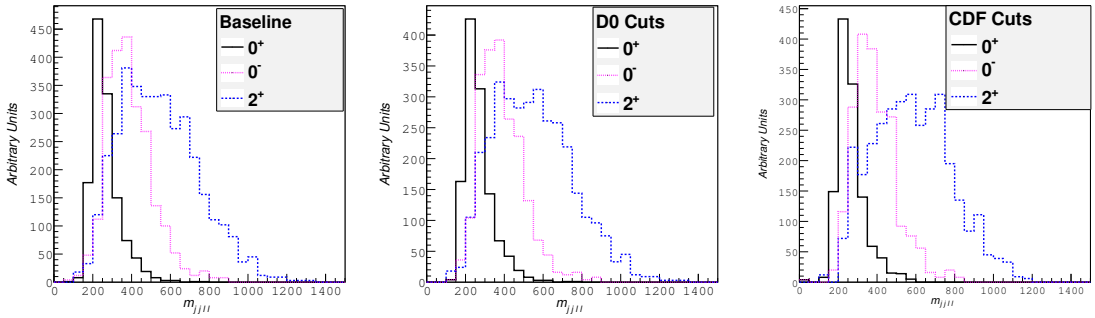

Figure 3. The effect of fast simulations of $Z \to \ell^+\ell^- + X \to \bar{b}b$ analyses with `Delphes`, using baseline (left panel), D0 [31] (centre panel) and CDF [32] cuts (right panel). The discrimination between different J^P assignments seen in figure 1 is maintained.

leptons of which at least one has $p_T > 15\,\text{GeV}$, and $|\eta_\ell| < 1.1$. Summing over the single- and double-tag categories, and adding the errors in quadrature, the number of events is 5.4 ± 0.3. The CDF [32] cuts we implement are more stringent. We ask for two or three jets, of which at least two have $p_T > 25\,\text{GeV}$, $|\eta_j|$ <2.5, and $m_{jj} > 25\,\text{GeV}$. Summing over all b-tagging categories, and adding the errors in quadrature, the number of events is 7.2 ± 0.6. Making fast simulations using `Delphes`, we find that the effects of these cuts on the M_{ZX} distributions are mild, so that the discrimination between the different quantum numbers assignments is maintained, as shown in the centre and right panels of figure 3, for the D0 and CDF experiments, respectively.

After the selection cuts, both collaborations perform a multivariate analysis. One can find in [31] a list of the variables used to train the random forest analysis, whose distribution depends on the quantum numbers of the candidate. The training was optimized for the 0^+ hypothesis, and this could impact the overall efficiency of the analysis in the cases of the 0^- and 2^+ assignments. To illustrate this point, we show in figure 4 the differences in the distribution of the difference in azimuthal angles, $\Delta\phi$, between the dijet and dilepton systems for the 0^+ and 2^+ spin assignments. However, the main discriminating variable is the dijet invariant mass, which is the same for all cases, so we expect only a moderate effect from the sensitivity of the angular variables to the X quantum numbers.

3.1.2 CDF $W^\pm \to \ell^\pm\nu + X \to \bar{b}b$ analysis

The analysis of this single-lepton channel has been published by CDF [33], and 25.3 ± 1.4 signal events were expected In the four two-jet categories. At the parton level, we impose the cuts $p_T^\ell > 20\,\text{GeV}$, $|\eta_\ell| < 2.5$, $p_T^j > 20\,\text{GeV}$, $|\eta_j|$ <2.5 and $\Delta R_{j\ell} > 0.5$. The CDF analysis requires exactly two or three jets with $p_T^j > 20\,\text{GeV}$ and $|\eta_j|$ <2. There is also a cut on missing energy that depends on the centrality of the lepton, with tighter cuts for forward leptons. If $|\eta_\ell| < 1.1$, the missing transverse energy $\not\!\!E_T$ is required to be above 20 GeV, increases to 25 GeV in the forward region. The selection cuts maintain the discrimination between different J^P assignments in the transverse mass variable

$$m_T^2 = (E_T^W + E_T^X)^2 - (\vec{p}_T^{\,W} + \vec{p}_T^{\,X})^2, \tag{3.1}$$

JHEP11(2012)134

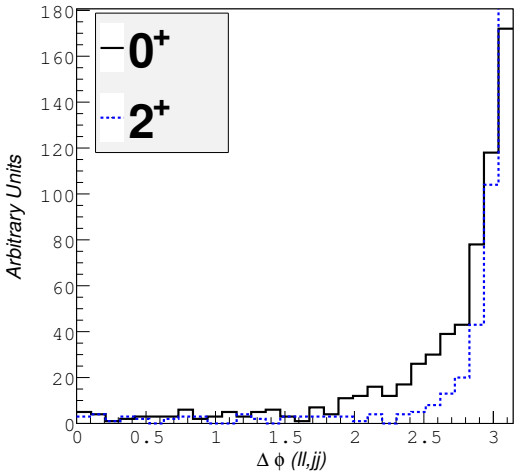

Figure 4. The distributions in the difference in azimuthal angles, $\Delta\phi$, between the dijet and dilepton systems in the TeVatron $Z \to \ell^+\ell^- + X \to \bar{b}b$ analyses, for the 0^+ and 2^+ spin assignments (black solid and blue dashed lines, respectively).

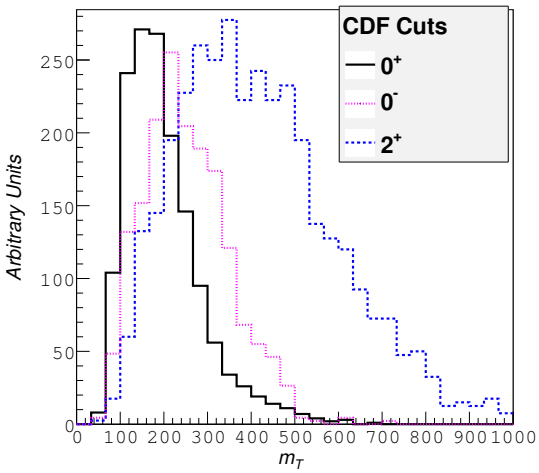

Figure 5. The effect of a fast simulation of the CDF $W^\pm \to \ell^\pm\nu + X \to \bar{b}b$ analysis [33] with `Delphes` on the transverse mass distributions for the different J^P assignments. The discrimination seen in figure 1 is maintained.

where the W transverse momentum is

$$\vec{p}_T^{\,W} = \vec{\not{E}}_T + \vec{p}_T^{\,\ell}, \tag{3.2}$$

as is shown in figure 5.

3.1.3 CDF and D0 $Z \to \bar{\nu}\nu + X \to \bar{b}b$ analyses

Both CDF [34] and D0 [35] have published analyses of events with $\not{E}_T$ and no detected leptons, which are sensitive to X production in association with $Z \to \nu\bar{\nu}$. We use `Delphes`

JHEP11(2012)134

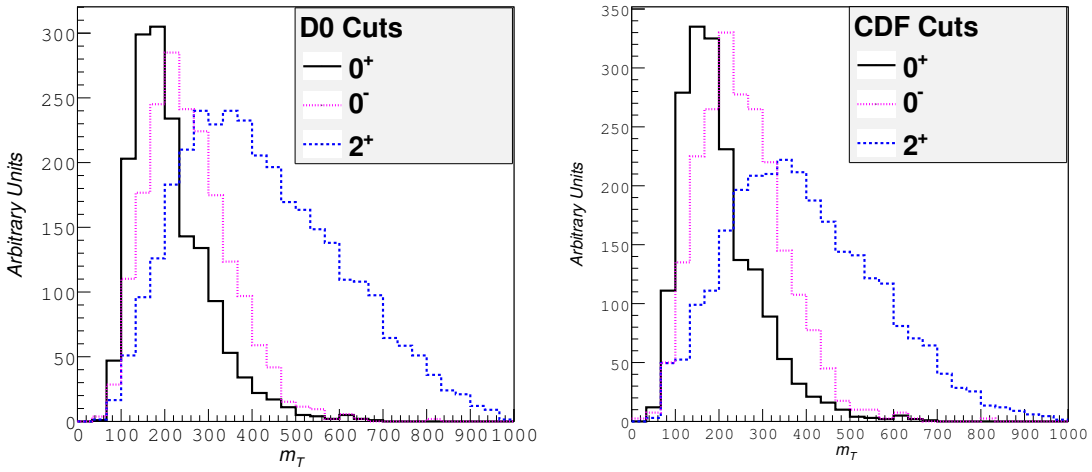

Figure 6. The effect of a fast simulation of the CDF [34] and D0 [35] $Z \to \bar{\nu}\nu + X \to \bar{b}b$ analyses with `Delphes` on the transverse mass distributions for the different J^P assignments. The discrimination between the different spin-parity assignments seen in figure 1 is maintained.

to reproduce the selection cuts in both analysis. In the case of D0, the relevant cuts are $p_T^j > 20\,\text{GeV}$, $|\eta_j| < 2.5$, $\Delta\phi_{j_1 j_2} < 165^0$, $\not{E}_T > 40\,\text{GeV}$, $H_T = |p_T^{j_1}| + |p_T^{j_2}| > 80\,\text{GeV}$ and $\mathcal{D} \equiv (|\Delta\phi_{\vec{p}_T,j_1}| + |\Delta\phi_{\vec{p}_T,j_1}|)/2 > \pi/2$. In the case of CDF, the cuts applied include jets with $p_T^j > 15\,\text{GeV}$ and $|\eta_j| < 2.4$, with the leading and subleading jets required to have $p_T > 25, 20\,\text{GeV}$, $|\eta_j| <2$ and $\Delta R_{jj} >0.8$, and at least one having $|\eta_j| <0.9$. In addition to these cuts, we apply the background rejection cuts $\not{E}_T > 35\,\text{GeV}$, $\Delta\phi(\vec{\not{E}}_T, E_T^{j_1}) \geqslant 1.5$ and $\Delta\phi(\vec{\not{E}}_T, E_T^{j_{2,3}}) \geqslant 0.4$.

We plot in figure 6 the distributions in the transverse mass variable

$$m_T^2 = (\not{E}_T + E_T^X)^2 - (\vec{\not{p}}_T + \vec{p}_T^X)^2, \tag{3.3}$$

where X corresponds to the two leading jet system. The number of signal events expected in all the D0 categories quoted as 59 ± 3 [35], whereas the number of events expected in the CDF analysis is 37, with no errors quoted in [34].

3.2 LHC $V + X \to \bar{b}b$ analyses

Both ATLAS [36] and CMS [37] have published the results of searches for associated $V+X$ production, so far establishing upper limits in the absence of a significant signal.

In simulating the ATLAS analysis with zero leptons, the parton-level cuts we use in our sample generation are $\not{E}_T > 120\,\text{GeV}$, $p_T > 80\,\text{GeV}$ for the leading jet, and $p_T^j > 20\,\text{GeV}$ for all other jets. We also use the cuts $\Delta\phi_{\not{E}_T,j} < \pi/2$ for the two leading jets. We follow the CMS analysis by including a selection for V and X decays with dijet pairs and V decays boosted in the transverse direction, via the cuts listed in table 1. Other cuts on combinations such as m_{jj} and $m_{\ell\ell}$ are automatically 100% efficient for the signal, as is the requirement for b-tagged jets. We note that jets are reconstructed using the anti-k_T algorithm with cut parameter 0.5.

JHEP11(2012)134

Variable	$W(\ell\nu)X$	$Z(\ell\ell)X$	$Z(\nu\nu)X$
p_T^{j1}	$> 30\,\text{GeV}$	$> 20\,\text{GeV}$	$> 80\,\text{GeV}$
p_T^{j2}	$> 30\,\text{GeV}$	$> 20\,\text{GeV}$	$> 20\,\text{GeV}$
p_T^{jj}	$> 120\,\text{GeV}$	–	$> 120\,\text{GeV}$
p_T^V	$> 120\,\text{GeV}$	$> 50\,\text{GeV}$	–
$\Delta\phi_{\not{E}_T,j}$	–	–	0.5
$\not{E}_T$	$> 35\,\text{GeV}$ (e)	–	$> 120\,\text{GeV}$

Table 1. Cuts used by CMS in their search for associated $V + X$ production. Note the selections for dijet pairs and V decays boosted in the transverse direction.

We display in figure 7 various kinematical distributions found after simulations of the ATLAS cuts (upper row) and the CMS cuts detailed in table 1 (lower row) for events with two, one and zero identified leptons (left, centre and right panels). In almost every case, we see that the distributions for the $0^+, 2^+$ and 0^- spin-parity assignments for the X particle are clearly distinguishable. The only exceptions are provided by the transverse mass distributions for the CMS analysis of one- and zero-lepton events, where we see that the 0^- and 0^+ cases are indistinguishable. This is a consequence of the boost requirements, which suppress low-mass $V + X$ combinations. These requirements also squeeze together the m_{VX} distributions for the two-lepton 0^+ and 0^-, though these are still distinguishable in principle.

4 Statistical procedure

The kinematic variable of interest for our analysis is $x \equiv M_{VX}$ or the related quantity M_T, and we can quantify the significance of the separation between different spin-parity hypothesis through the use of a likelihood for the distribution in x. Since we are dealing with low statistics we consider an unbinned likelihood in the spirit of [38].

The likelihood of a single event x_i, for a spin-parity hypothesis $s = 0^+, 0^-, 2^+$, is given by a probability density function $\text{pdf}_s(x_i)$. This pdf is a normalized, high-statistics Monte Carlo histogram that takes into account detector acceptance effects and cuts on the distribution of the kinematic variable x. The full likelihood for x is then obtained by multiplying the pdf for each event i:

$$\mathcal{L}_s = \prod_{i=1}^{M} \text{pdf}_s(x_i)\,. \tag{4.1}$$

We follow the Neyman-Pearson approach in using the log-likelihood ratio for our test statistic, defined as

$$\Lambda = -2\ln\left(\frac{\mathcal{L}_A}{\mathcal{L}_B}\right)\,. \tag{4.2}$$

The separation significance between two spin-parity hypotheses A and B can be estimated by generating a large number of toy experiments to obtain a distribution in Λ. If the

JHEP11(2012)134

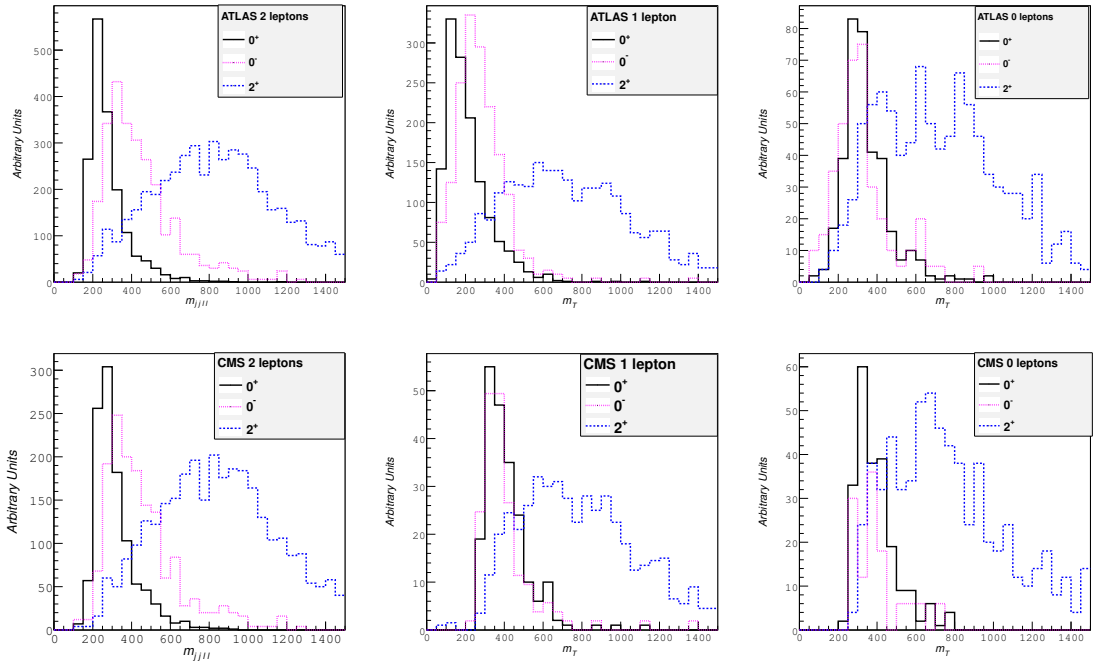

Figure 7. Kinematical distributions for the 7-TeV ATLAS (upper row) and CMS (lower row) $V+X \to \bar{b}b$ analyses in the two-, one- and zero-lepton cases (left, centre and right panels, respectively).

toys are generated for hypothesis A, then the distribution of Λ, $f_A(\Lambda)$, will be centered around a negative mean value. Conversely, for toys generated according to hypothesis B the Λ distribution $f_B(\Lambda)$ will be centered around a positive mean, with the tails of the two distributions f_A and f_B overlapping to a certain extent.

For a given observed $\Lambda_{\rm obs}$, the probability of getting a more extreme value of Λ than the one observed assuming hypothesis A is

$$\alpha = \begin{cases} \frac{1}{N}\int_{\Lambda_{\rm obs}}^{\infty} f_A(\Lambda)d\Lambda & \Lambda_{\rm obs} \geq \Lambda_{\rm mean} \\ \frac{1}{N}\int_{-\infty}^{\Lambda_{\rm obs}} f_A(\Lambda)d\Lambda & \Lambda_{\rm obs} < \Lambda_{\rm mean} \end{cases} \tag{4.3}$$

where $N = \int_{-\infty}^{\infty} f_A(\Lambda)d\Lambda$. A similar definition can be given for the probability β assuming hypothesis B instead. These can be identified with the p-values quantifying the agreement between the observed data and the hypotheses.

We may restrict the definition of α and β to be always the integral towards the right and left tail end of the distribution, respectively. Then α is also defined as the "type I" error, namely the probability of rejecting hypothesis A given that it is true, and β is the "type II" error, namely the probability of wrongly accepting hypothesis A given that B is actually true. The "power" of the test is $1-\beta$, so that a high probability of getting a type II error corresponds to a test with weak power.

There are two ways of reporting the expected significance, reflecting different underlying philosophies. The first takes an asymmetric approach to the two hypotheses: the

JHEP11(2012)134

mean value of Λ under hypothesis A is the value of $\Lambda_{\rm obs}$ that an experiment is expected to measure if hypothesis A is true, and one may quote the p-value β, the level at which we will then be able to exclude hypothesis B. By randomly sampling $\Lambda_{\rm obs}$ from f_A, one can give one-sigma bands for the expected significance for β. In this approach the value of α and β defined as the acceptance limit is fixed (for example to 0.05) and we seek to minimize β, the type II error. The second approach instead treats the two hypotheses equally by defining the acceptance region for hypothesis A (B) as lying to the left (right) of $\Lambda_{\rm cutoff}$ respectively, where $\Lambda_{\rm cutoff}$ is the value of Λ for which $\alpha = \beta$. Thus, whatever the value of $\Lambda_{\rm obs}$, the significance with which one hypothesis can be considered excluded and the other accepted is α $(= \beta)$.

It is clear from these two definitions of expected significance that, given a distribution of Λ for the two hypotheses, the second (symmetric) approach will yield a more conservative significance than the first (asymmetric method). Since it is also the more objective method, below we quote this symmetric approach for the significance.

The significance α is usually translated into n standard deviations by finding the equivalent area under a standard Gaussian distribution:[2]

$$\alpha = \frac{1}{\sqrt{2\pi}} \int_n^\infty e^{-\frac{x^2}{2}} dx \,. \tag{4.4}$$

For example, $\alpha = 0.05$ corresponds to $n = 1.64$, and the discovery standard of $n = 5$ corresponds to $\alpha = 2.87 \times 10^{-7}$.

5 Analysis using 'toy' experiments

We evaluated the expected separation significance using both the symmetric and the asymmetric method,[3] by generating 100 'toy' experiments corresponding to each of the analyses discussed above, namely the CDF, ATLAS and CMS 0-, 1- and 2-lepton analyses, and the D0 0- and 2-lepton analyses. These toys are designed to reproduce the statistics found in the corresponding analyses after implementing the event selections and cuts. We have checked in specific cases that the separation significances quoted below are quite insensitive to the number of 'toys' beyond 100. In modelling each analysis, we neglect the contaminations by backgrounds: their simulation would be more complicated and take us beyond the scope of this work. We note that the backgrounds in the TeVatron analyses are in any case very small in the bins with $\log_{10}(s/b) > -1.5$ [3]. The backgrounds in the LHC analyses are currently larger, but we expect them to decrease as the analyses are refined.

Figure 8 illustrates how these toys can be used to estimate the statistical separations between a pair of J^P hypotheses that can be achieved, using the example of the D0 zero-, one- and two-lepton analyses. A set of 100 'toy' experiments was generated for each of these analyses, and the results combined. The horizontal axis is the symmetric test

[2] This is the one-sided definition most commonly used in the literature, as opposed to the two-sided convention sometimes seen, which generally yields a higher number of standard deviations for the same p-value.

[3] Though below we quote results only for the former, more conservative, approach.

JHEP11(2012)134

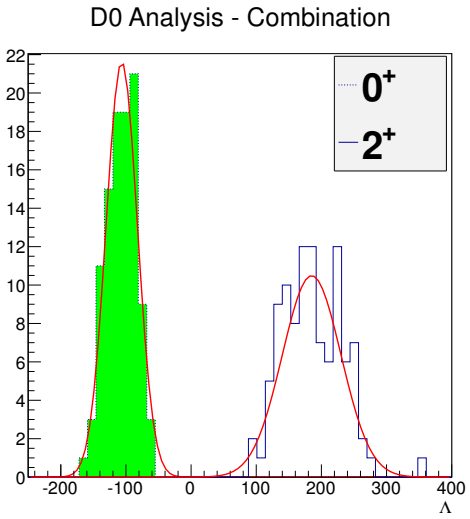

Figure 8. An example of the statistical separation that could be achieved between the spin-parity assignments $J^P = 0^+$ and 2^+. It is based on a combination of sets of 100 'toy' experiments simulating the D0 zero-, one- and two-lepton analysis separately, each with a number of events surviving the experimental cuts that is similar to that found in the D0 analysis.

statistic $\Lambda \equiv -2\ln(\mathcal{L}_A/\mathcal{L}_B)$ (4.2). The separation between the distributions generated for the $J^P = 0^+$ and 2^+ hypotheses (green shaded dotted blue and open blue solid histograms, respectively) is clear.

Table 2 summarizes the statistical separations we find for each TeVatron and LHC analysis between the 0^+ and 2^+ hypotheses and between the 0^+ and 0^- hypotheses (in parentheses). As one would expect from the invariant-mass distributions shown earlier, the statistical separation between the 0^+ and 2^+ hypotheses is generally stronger than that between the 0^+ and 0^- hypotheses. Also shown are the separation significances we find for the combinations of analyses in the TeVatron experiments. We note that in these experiments the approximate overall significance of their evidence for X production in association with vector bosons [3] $\sim 3\sigma$, so results above this level for the separation significance are only formal. In the cases of the LHC experiments, we quote results only for the two-lepton analyses, as the separation significances we find in their one- and zero-lepton analyses are much lower. Since the backgrounds in the LHC experiments are currently large compared with any signals, our results (which assume negligible backgrounds) are not directly applicable at present. However, we expect the signal/background ratios to increase as the analyses progress, and the results in table 2 suggest levels of separation to which improved analyses could aspire.

In the cases of the LHC analyses, we have also generated toys simulating the larger numbers of signal events that will become available in the future, with the results illustrated in figure 9 (neglecting backgrounds, as before). The left panel shows how the statistical significance in the CMS two-lepton analysis, in numbers of σ, of the separations between the 0^+ and 2^+ hypotheses (upper points and red line to guide the eye) and between the 0^+ and 0^- hypotheses (lower points and blue line) would increase with the number of

JHEP11(2012)134

Experiment	Category	Hypothesis A	Hypothesis B	Significance in σ
CDF	0l	0^+	$2^+(0^-)$	3.7 (1.3)
	1l	0^+	$2^+(0^-)$	2.5 (1.0)
	2l	0^+	$2^+(0^-)$	1.4 (0.78)
	Combined	0^+	$2^+(0^-)$	4.8 (1.6)
D0	0l	0^+	$2^+(0^-)$	3.5 (1.2)
	2l	0^+	$2^+(0^-)$	1.8 (1.2)
	Combined	0^+	$2^+(0^-)$	4.0 (1.6)
ATLAS	2l	0^+	$2^+(0^-)$	2.4 (1.1)
CMS	2l	0^+	$2^+(0^-)$	2.3 (0.70)

Table 2. The separation significances between different J^P hypotheses estimated for each Tevatron and LHC experiment, using in each case 100 'toy' experiments with similar event numbers to the data, using the symmetric method of hypothesis testing described in the text.

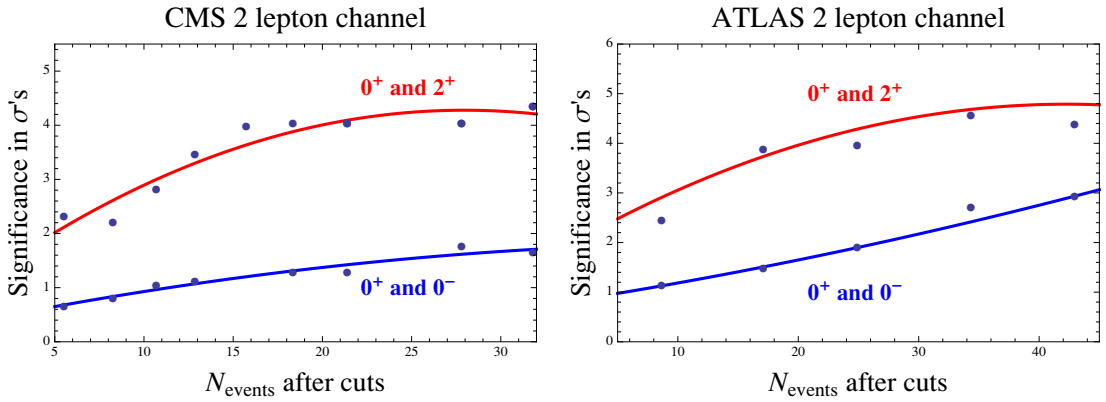

Figure 9. The variation in the significance of the statistical separation obtainable as a function of the number N of events surviving the CMS (left) and ATLAS (right) experimental event selections and cuts for two-lepton events, for distinguishing between 0^+ and 2^+ (upper points and red lines) and between 0^+ and 0^- (lower points and blue lines).

signal events N surviving the experimental selection and cuts. The right panel shows a similar analysis for the ATLAS two-lepton analysis. We see again that it will be easier to discriminate between the 0^+ and 2^+ hypotheses than between the 0^+ and 0^- hypotheses, and that the hypotheses can be distinguished cleanly if the backgrounds can be suppressed.

6 Conclusions

We have shown in this paper that the invariant mass distributions for $V+X$ combinations, M_{VX}, are theoretically very different for the $J^P = 0^+, 0^-$ and 2^+ assignments for the new boson with mass $\sim 125\,\text{GeV}$ recently discovered by the ATLAS and CMS Collabora-

JHEP11(2012)134

tions [1, 2]. Making simulations using PYTHIA and Delphes, we have also shown that these differences survive the experimental event selections and cuts in searches for X production in association with two-, one- and zero-lepton decays of the heavy vector bosons Z and W. We have also used simulated 'toy' experiments to estimate the statistical separations that could in principle be attained by the CDF, D0, ATLAS and CMS experiments if the experimental backgrounds were negligible.

In the case of the TeVatron experiments that have already provided evidence for 'Higgs'-strahlung [3], our analysis indicates that the data currently available should be able to discriminate between the 0^+ and either the 2^+ or 0^- hypotheses with high significance, assuming that the backgrounds are small. Indications are that the backgrounds in the invariant mass range expected under the 2^+ hypothesis should indeed be very small, as we have illustrated with one example that also indicates that the M_{ZX} distribution from a 0^- signal should also be quite different. A more complete evaluation of the signal/background discrimination under different J^P hypotheses requires more understanding of their MVA analyses than was provided in [3]. The 'Higgs'-strahlung analyses in the LHC experiments have not yet been optimized, and currently do not show evidence for a signal, but our analysis show what statistical separations might be attainable with increased data sets and reduced backgrounds.

Analyses of the possible backgrounds go beyond the scope of this paper. Following this pioneering proposal, we expect that the experimental analyses will evolve, at which stage a more detailed exploration of the signal/background separations would become appropriate. However, we think that our analysis already demonstrates the potential of M_{VX} measurements to provide valuable insight into the possible J^P assignment of the X particle. It may well be that its J^P will be determined by a combination of different measurements that each make contributions to the global likelihood. In this perspective, we hope that the the M_{VX} measurements proposed here will play useful roles.

Acknowledgments

We thank Ricky Fok for valuable discussions on related subjects. The work of JE and TY was supported partly by the London Centre for Terauniverse Studies (LCTS), using funding from the European Research Council via the Advanced Investigator Grant 267352. The work of DSH was supported partly by Korea Foundation for International Cooperation of Science & Technology (KICOS) and Basic Science Research Programme through the National Research Foundation of Korea (2012-0002959). The authors thank CERN for kind hospitality, and TY additionally thanks Prof. T. Kobayashi and the Bilateral International Exchange Program of Kyoto University for kind hospitality during the completion of this work.

JHEP11(2012)134

References

[1] ATLAS collaboration, G. Aad et al., *Observation of a new particle in the search for the Standard Model Higgs boson with the ATLAS detector at the LHC*, *Phys. Lett.* **B 716** (2012) 1 [arXiv:1207.7214] [INSPIRE].

[2] CMS collaboration, S. Chatrchyan et al., *Observation of a new boson at a mass of 125 GeV with the CMS experiment at the LHC*, *Phys. Lett.* **B 716** (2012) 30 [arXiv:1207.7235] [INSPIRE].

[3] CDF, D0 collaboration, T. Aaltonen et al., *Evidence for a particle produced in association with weak bosons and decaying to a bottom-antibottom quark pair in Higgs boson searches at the Tevatron*, *Phys. Rev. Lett.* **109** (2012) 071804 [arXiv:1207.6436] [INSPIRE].

[4] J. Ellis and T. You, *Global analysis of the Higgs candidate with mass* ~ 125 *GeV*, *JHEP* **09** (2012) 123 [arXiv:1207.1693] [INSPIRE].

[5] S. Choi, D.J. Miller, M. Muhlleitner and P. Zerwas, *Identifying the Higgs spin and parity in decays to Z pairs*, *Phys. Lett.* **B 553** (2003) 61 [hep-ph/0210077] [INSPIRE].

[6] K. Odagiri, *On azimuthal spin correlations in Higgs plus jet events at LHC*, *JHEP* **03** (2003) 009 [hep-ph/0212215] [INSPIRE].

[7] C. Buszello, I. Fleck, P. Marquard and J. van der Bij, *Prospective analysis of spin- and CP-sensitive variables in* $H \to ZZ \to l_1^+ l_1^- l_2^+ l_2^-$ *at the LHC*, *Eur. Phys. J.* **C 32** (2004) 209 [hep-ph/0212396] [INSPIRE].

[8] A. Djouadi, *The anatomy of electro-weak symmetry breaking. I: The Higgs boson in the standard model*, *Phys. Rept.* **457** (2008) 1 [hep-ph/0503172] [INSPIRE].

[9] C. Buszello and P. Marquard, *Determination of spin and CP of the Higgs boson from WBF*, hep-ph/0603209 [INSPIRE].

[10] A. Bredenstein, A. Denner, S. Dittmaier and M. Weber, *Precise predictions for the Higgs-boson decay* $H \to WW/ZZ \to 4$ *leptons*, *Phys. Rev.* **D 74** (2006) 013004 [hep-ph/0604011] [INSPIRE].

[11] P. Bhupal Dev, A. Djouadi, R. Godbole, M. Muhlleitner and S. Rindani, *Determining the CP properties of the Higgs boson*, *Phys. Rev. Lett.* **100** (2008) 051801 [arXiv:0707.2878] [INSPIRE].

[12] R.M. Godbole, D.J. Miller, and M.M. Muhlleitner, *Aspects of CP-violation in the H ZZ coupling at the LHC*, *JHEP* **12** (2007) 031 [arXiv:0708.0458] [INSPIRE].

[13] K. Hagiwara, Q. Li and K. Mawatari, *Jet angular correlation in vector-boson fusion processes at hadron colliders*, *JHEP* **07** (2009) 101 [arXiv:0905.4314] [INSPIRE].

[14] Y. Gao et al., *Spin determination of single-produced resonances at hadron colliders*, *Phys. Rev.* **D 81** (2010) 075022 [arXiv:1001.3396] [INSPIRE].

[15] A. De Rujula, J. Lykken, M. Pierini, C. Rogan and M. Spiropulu, *Higgs look-alikes at the LHC*, *Phys. Rev.* **D 82** (2010) 013003 [arXiv:1001.5300] [INSPIRE].

[16] C. Englert, C. Hackstein and M. Spannowsky, *Measuring spin and CP from semi-hadronic ZZ decays using jet substructure*, *Phys. Rev.* **D 82** (2010) 114024 [arXiv:1010.0676] [INSPIRE].

[17] U. De Sanctis, M. Fabbrichesi and A. Tonero, *Telling the spin of the 'Higgs boson' at the LHC*, *Phys. Rev.* **D 84** (2011) 015013 [arXiv:1103.1973] [INSPIRE].

JHEP11(2012)134

[18] V. Barger and P. Huang, *Higgs boson finder and mass estimator: The Higgs boson to WW to leptons decay channel at the LHC*, *Phys. Rev.* **D 84** (2011) 093001 [arXiv:1107.4131] [INSPIRE].

[19] J. Ellis and D.S. Hwang, *Does the 'Higgs' have Spin Zero?*, *JHEP* **09** (2012) 071 [arXiv:1202.6660] [INSPIRE].

[20] S. Bolognesi et al., *On the spin and parity of a single-produced resonance at the LHC*, arXiv:1208.4018 [INSPIRE].

[21] R. Boughezal, T.J. LeCompte and F. Petriello, *Single-variable asymmetries for measuring the 'Higgs' boson spin and CP properties*, arXiv:1208.4311 [INSPIRE].

[22] D. Stolarski and R. Vega-Morales, *Directly measuring the tensor structure of the scalar coupling to gauge bosons*, arXiv:1208.4840 [INSPIRE].

[23] D.J. Miller, S. Choi, B. Eberle, M. Muhlleitner and P. Zerwas, *Measuring the spin of the Higgs boson*, *Phys. Lett.* **B 505** (2001) 149 [hep-ph/0102023] [INSPIRE].

[24] K. Hagiwara, J. Kanzaki, Q. Li and K. Mawatari, *HELAS and MadGraph/MadEvent with spin-2 particles*, *Eur. Phys. J.* **C 56** (2008) 435 [arXiv:0805.2554] [INSPIRE].

[25] J. Alwall, M. Herquet, F. Maltoni, O. Mattelaer and T. Stelzer, *MadGraph 5: Going Beyond*, *JHEP* **06** (2011) 128 [arXiv:1106.0522] [INSPIRE].

[26] T. Sjöstrand, S. Mrenna and P.Z. Skands, *PYTHIA 6.4 Physics and Manual*, *JHEP* **05** (2006) 026 [hep-ph/0603175] [INSPIRE].

[27] S. Ovyn, X. Rouby and V. Lemaitre, *DELPHES, a framework for fast simulation of a generic collider experiment*, arXiv:0903.2225 [INSPIRE].

[28] N.D. Christensen and C. Duhr, *FeynRules — Feynman rules made easy*, *Comput. Phys. Commun.* **180** (2009) 1614 [arXiv:0806.4194] [INSPIRE].

[29] C. Degrande et al., *UFO — The Universal FeynRules Output*, *Comput. Phys. Commun.* **183** (2012) 1201 [arXiv:1108.2040] [INSPIRE].

[30] R. Fok, C. Guimaraes, R. Lewis and V. Sanz, *It is a Graviton! or maybe not*, arXiv:1203.2917 [INSPIRE].

[31] D0 collaboration, V.M. Abazov et al., *Search for the standard model Higgs boson in* $ZH \to \ell^+\ell^- b\bar{b}$ *production with the D0 detector in* $9.7\,fb^{-1}$ *of* $p\bar{p}$ *collisions at* $\sqrt{s} = 1.96\ TeV$, *Phys. Rev. Lett.* **109** (2012) 121803 [arXiv:1207.5819] [INSPIRE].

[32] CDF collaboration, T. Aaltonen et al., *Search for the standard model Higgs boson decaying to a bb pair in events with two oppositely-charged leptons using the full CDF data set*, *Phys. Rev. Lett.* **109** (2012) 111803 [arXiv:1207.1704] [INSPIRE].

[33] CDF collaboration, T. Aaltonen et al., *Search for the standard model Higgs boson decaying to a bb pair in events with one charged lepton and large missing transverse energy using the full CDF data set*, *Phys. Rev. Lett.* **109** (2012) 111804 [arXiv:1207.1703] [INSPIRE].

[34] CDF collaboration, T. Aaltonen et al., *Search for the standard model Higgs boson decaying to a* $b\bar{b}$ *pair in events with no charged leptons and large missing transverse energy using the full CDF data set*, *Phys. Rev. Lett.* **109** (2012) 111805 [arXiv:1207.1711] [INSPIRE].

[35] D0 collaboration, V.M. Abazov et al., *Search for the standard model Higgs boson in the* $ZH \to \nu\bar{\nu}b\bar{b}$ *channel in* $9.5\,fb^{-1}$ *of* $p\bar{p}$ *collisions at* $\sqrt{s} = 1.96\ TeV$, *Phys. Lett.* **B 716** (2012) 285 [arXiv:1207.5689] [INSPIRE].

JHEP11(2012)134

[36] ATLAS collaboration, G. Aad et al., *Search for the Standard Model Higgs boson produced in association with a vector boson and decaying to a b-quark pair with the ATLAS detector*, arXiv:1207.0210 [INSPIRE].

[37] CMS collaboration, S. Chatrchyan et al., *Search for the standard model Higgs boson produced in association with W or Z bosons, and decaying to bottom quarks for ICHEP 2012*, http://cdsweb.cern.ch/record/1460692/files/HIG-12-019-pas.pdf.

[38] R. Cousins, J. Mumford, J. Tucker and V. Valuev, *Spin discrimination of new heavy resonances at the LHC*, *JHEP* **11** (2005) 046 [INSPIRE].

JHEP11(2012)134